

## Electronic Supplementary Information

### Digital microfluidic meter-on-chip

Zecong Fang<sup>a</sup>, Yi Ding<sup>ab</sup>, Zhichao Zhang<sup>a</sup>, Hao Wang<sup>c</sup>, Zuankai Wang<sup>d</sup>, Fei Wang<sup>e</sup> and Tingrui Pan<sup>\*ab</sup>

<sup>a</sup> Micro-Nano Innovations (MiNI) Laboratory, Department of Biomedical Engineering, University of California, Davis, CA, 95616, USA

<sup>b</sup> Department of Electrical and Computer Engineering, University of California, Davis, CA, 95616, USA.

<sup>c</sup> Department of Energy and Resources Engineering, Peking University, Beijing, 100871, China.

<sup>d</sup> Department of Mechanical Engineering, City University of Hong Kong, Hong Kong, 999077, China.

<sup>e</sup> Department of Electrical and Electronic Engineering, Southern University of Science and Technology, Shenzhen, 518055, China.

#### 1. Fabrication process of the DMC devices

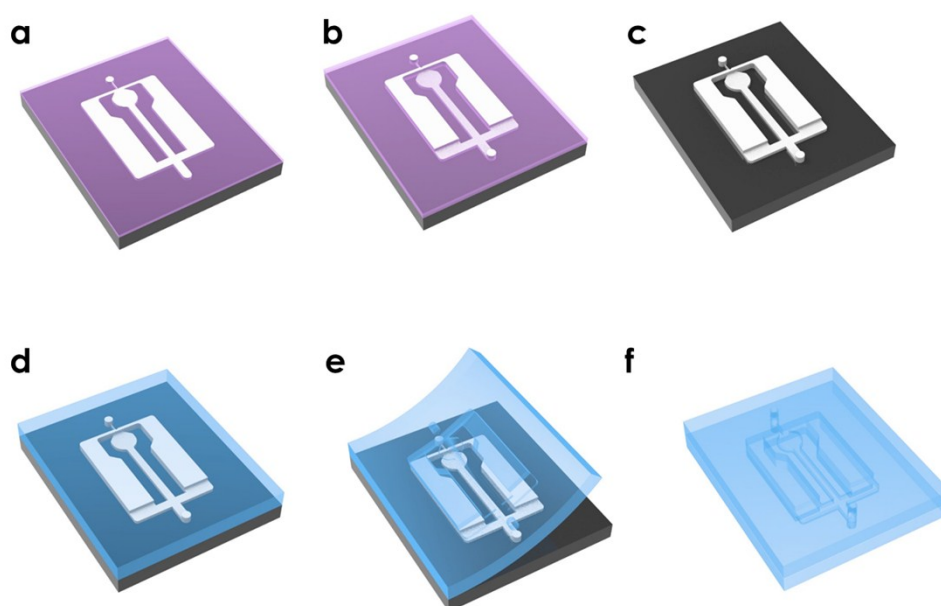


Fig. S1 Layer-by-layer fabrication of the DMC devices. Spin coating, UV light exposure and baking of a) first layer and b) second layer. c) Master after development. d) Molding of PDMS. e) Peel-off of PDMS f) Plasma bonding to form the DMC device.

## 2. Electric circuit for detection of flow digitization process in DMC devices

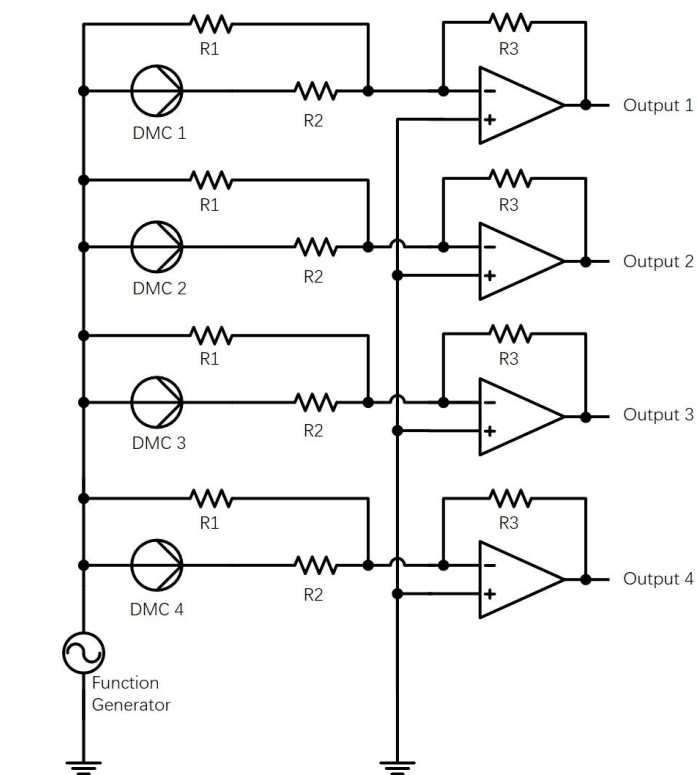


Fig. S2 Schematic of the electric circuit for the DMC devices.

## 3. Smartphone snapshots for the detection of flow digitization process in DMC devices

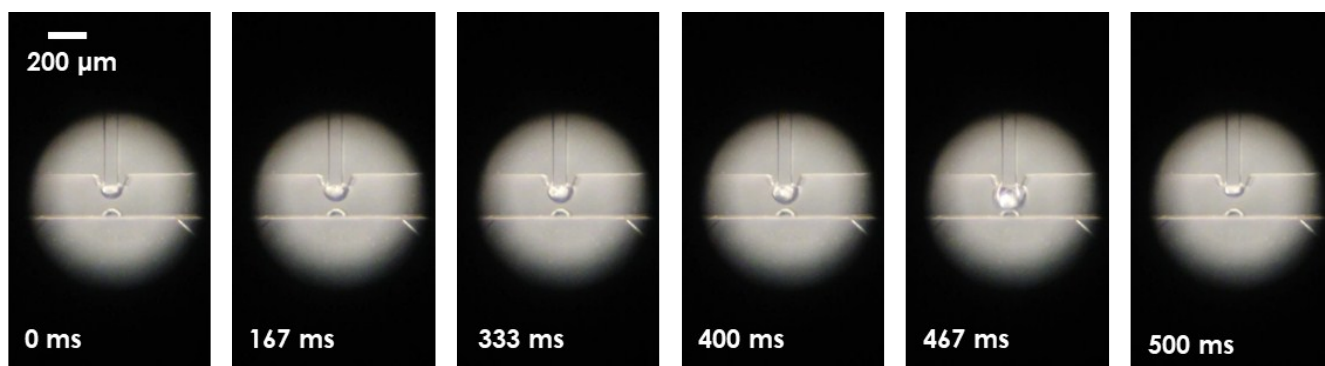


Fig. S3 Snapshots of the emergence, coalescence and pinch-off of the droplet with a smartphone camera at 30fps and flowrate of 300nL/min. The small stationary droplet is attached to the side wall of the air chamber and it is used as an indicator of the air chamber.

#### 4. Influences of air-buffered chamber (ABC)

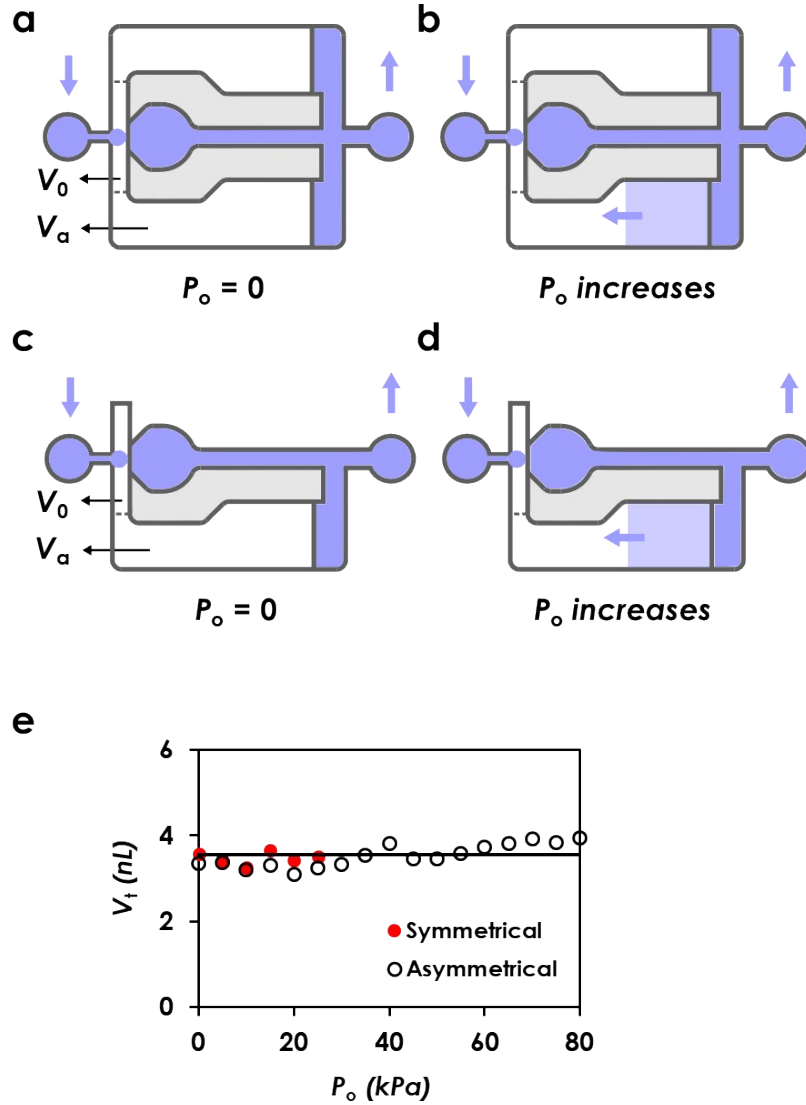


Fig. S4 Illustration of the moving of buffering interface inside the air chamber when outlet pressure is elevated at a flowrate of  $5\mu\text{L}/\text{min}$ , in a-b) symmetrical and c-d) asymmetrical air chamber architecture. e) Independence of droplet transfer volume with outlet pressure.

#### 5. Derivation of maximum outlet pressure In DMC devices

In particular, the air chamber can be divided into two zones, namely a buffering zone (with a volume of  $V_a$ ) and a dead volume zone (with a volume of  $V_0$ ), separated by a dash line as illustrated in **Fig. S4a**. Originally, the outlet pressure and the air chamber pressure are both equal to atmospheric pressure ( $P_0$ ). When the outlet pressure increases, the air inside is compressed by the buffering air-liquid interface. Assume that the buffering interface is initially located at the borderline of the liquid reservoir and the air chamber, the total volume of air at the beginning would be  $V_0 + V_a$ . Upon compression, part of the air chamber is filled up with liquid (with a volume of  $V$ ). Therefore, the volume of air reduces to  $V_0 + V_a - V$ , and the pressure inside the air chamber

increases to  $P_a = \left(1 + \frac{V}{V_0 + V_a - V}\right)P_0$ , assuming the compression process is isothermal. As the volume of the buffering zone is

$V_a$ , the maximum possible absolute pressure in the air chamber would be  $P_{a,max} = (1 + V_a/V_0)P_0$ , and the equivalent maximum gauge pressure would be  $(V_a/V_0)P_0$ . It is worth noting that in the symmetrical DMC configuration as shown in the **Figs. S4a-b**, once the buffering interface in either side of the chamber approaches the dead volume zone, the DMC fails to work, and at that moment, the other side of the air chamber is not filled up with any liquid. As a result, for the symmetrical configuration of DMC,

the theoretical maximum pressure is expected to be  $P_{a,max} = \frac{V_0 + V_a}{V_0 + 0.5V_a}P_0$ . If the dead volume  $V_0$  is significantly smaller than the buffering volume  $V_a$ , the maximum pressure will approach  $2P_0$  (equivalent gauge pressure of  $P_0$ ). To extend the working pressure range, an asymmetrical configuration of DMC can be implemented, as shown in **Figs. S4c-d** and the maximum pressure for this asymmetrical configuration would be  $P_{a,max} = (1 + V_a/V_0)P_0$ , as aforementioned. This threshold value also defines the maximum failure pressure for DMC devices and indicates that the working pressure range of DMC devices can be adjusted by tuning the volume ratio between the buffering zone and the dead volume zone.

## 6. Movie S1: High-speed imaging of the droplet emergence, coalescence and pinch-off in DMC devices.

The video was captured at 10,000fps and played back at 30fps. The nozzle width and nozzle height are both 100 $\mu$ m and the

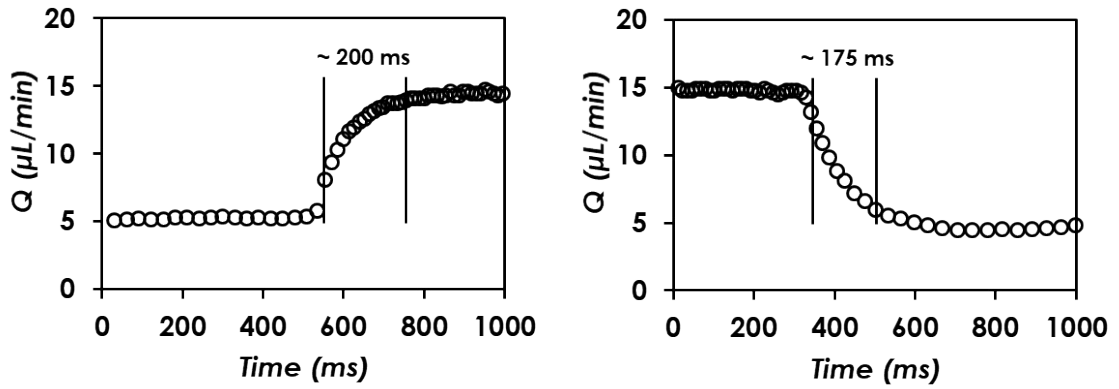


Fig. S5 Dynamic response of DMC devices with nozzle width of 100 $\mu$ m and separation distance of 150 $\mu$ m. The response time is determined to be approximately 200ms and 175ms from the dynamic response curve, respectively.

separation distance is 150 $\mu$ m. The flowrate is 10 $\mu$ L/min.

## 7. Smartphone snapshots for the detection of flow digitization process in DMC devices